# Disposable Planar Microwave Sensor for Real-time Monitoring of Lubricant Depletion on Lubricant-infused Coated Medical Implants

Amirhossein Yazdanicherati [1], Erin L. Roberts [2], Maryam Badv [2, 3], Zahra Abbasi [1]
[1]Department of Electrical and Software Engineering, Schulich School of Engineering, University of Calgary, Canada
[2] Department of Biomedical Engineering,Schulich School of Engineering, University of Calgary, Canada
[3]Libin Cardiovascular Institute, Canada
{amirhossein.yazdanic, erin.roberts2, maryam.badv, zahra.abbasi}@ucalgary.ca

***Abstract*— This paper proposes a passive disposable planar microwave resonator sensor for real-time monitoring of lubricant depletion on lubricant-infused surfaces. These surface coatings offer a state-of-the-art solution to minimize the complications associated with medical implants caused by non-specific adhesion of blood components and bacteria. The stability of the lubricant layer determines the function of the lubricant-infused coating. It is an essential factor that needs to be considered when applying these coatings on medical implants. The proposed passive split-ring resonator (SRR)-based sensor introduces the real-time monitoring of the thickness and evaporation rate of the lubricant layer. The performance and sensitivity of the sensor have been verified in simulation and measurement. The design is capable of monitoring lubricant presence in porous and no-porous surfaces. Additionally, using this SRR-based sensor, the drastic depletion zones on the surface can be detected.**

***Keywords*— Microwave sensors, lubricant-infused surface, split-ring resonators, non-specific adhesion, disposable sensor.**

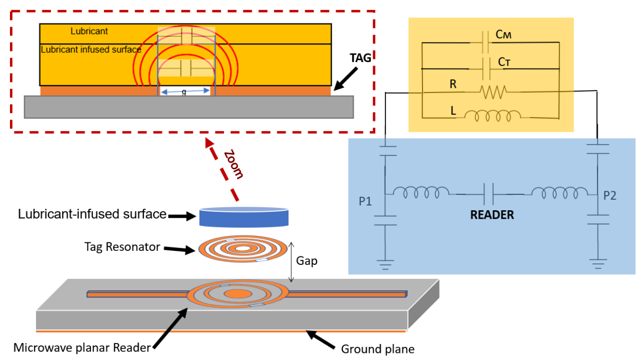


Fig. 1. The schematic of lubricant evaporation monitoring on the surface using microwave sensor and lumped-element equivalent circuit. The setup consists of a microwave reader, tag resonator, and lubricant-infused surface.

## I. Introduction

Device-associated clot formation and bacteria adhesion are ongoing problems with medical implants and pose a significant burden on the healthcare system. Lubricant-infused surfaces (LIS) have recently gained attention as a promising surface coating to prevent non-specific adhesion on bio-interfaces and medical implants [1]. LIS can repel biological liquids through the presence of a thin lubricant layer integrated within a solid substrate, creating a mobile super-repellent liquid interface. The stability of the lubricant layer under different conditions (e.g., open-air conditions) and when using different solid substrates (e.g., non-porous and porous substrates) is an important factor that affects the function of the coating and needs to be considered [2]. Several approaches have been used to measure the evaporation rate of the lubricant layer, including measuring the volume of the lubricant before and after predetermined time points [3], measuring the contact angle of a water droplet on the surface over time [4], [5], and microscopic techniques [6]. However, these approaches suffer from limitations such as requiring bulky and expensive systems and lacking real-time monitoring features. Therefore, designing a real-time, compact sensor-based technology that measures the evaporation rate of the lubricant layer on surfaces could be highly beneficial. Microwave sensors offer a solid, robust solution for wireless and noncontact sensing applications. A planar split-ring resonator (SRR)-based structures are among the most interesting structures for sensing applications due to their compact structure, simple mass production of the design, and easy integration with Lab-on-a-chip technologies [7]. SRR sensors have shown great enabling potential in various applications, such as biomedicine and biochemistry [8]. More importantly, their noncontact and real-time detection capability makes them a suitable candidate for blood-contacting medical applications.

Here, a sensor-based approach is proposed for real-time monitoring of lubricant evaporation on lubricant-infused surfaces using coupled split-ring resonator sensor. The design consists of a tag SRR as the main sensing interface coupled to a planar reader [7]. The tag resonator is combined with the surface under the test as a disposable monitoring device while communicating the lubricant evaporation on the LIS to the wireless reader. This microwave sensing approach offers an inexpensive, portable, quantitative, and highly sensitive solution for precise measurement of the presence of the lubricant layer. Flat (non-porous) and porous hydrogel substrates were tested to investigate the differences in the lubricant evaporation rate. Section II presents the sensor design process and simulation, and the measurement results are described in Section III.

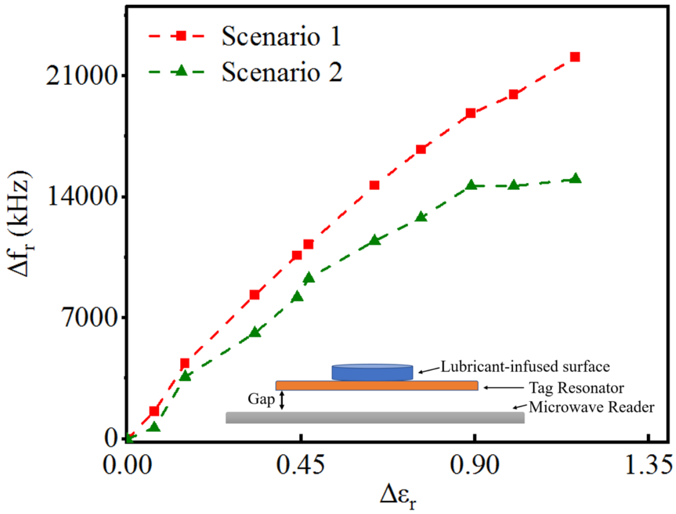


Fig. 2. Schematic of the sensor setup, the absolute value of resonance frequency shift for two different Lubricant-infused surfaces with the same $\varepsilon_r$ changes.

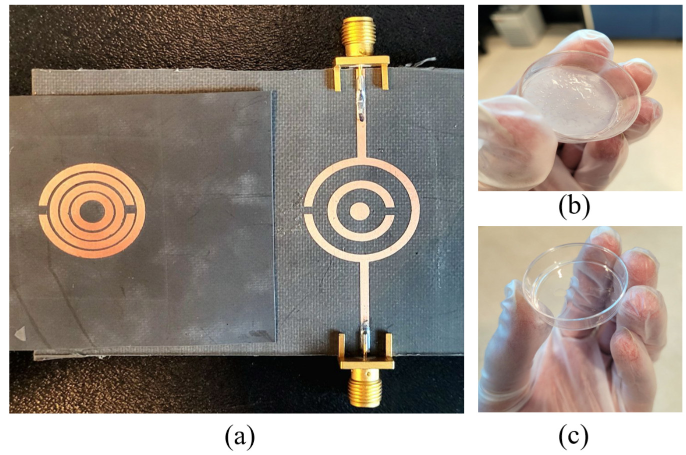


Fig. 3. (a) Fabricated tag and microwave planar reader, (b) porous lubricant-infused surface, (c) non-porous lubricant-infused surface.

## II. Sensor design and simulation

Fig. 1 summarizes the proposed idea and its equivalent circuit model. As shown in Fig. 1, the tag resonator is coupled to a microwave planar reader with the full ground plane on the bottom to maximize the electromagnetic coupling. The tag is integrated with a container that is a lubricant-infused surface (e.g., a flat non-porous petri dish) and wirelessly communicates the lubricant evaporation trend to the reader. Separating the tag from the same plane as the 2-port planar reader empowers this structure to be used as a disposable monitoring device for surface monitoring applications. The strong coupling between the tag and the reader enables the proposed design to be highly sensitive and detect variations in ultra-thin layers of lubricants on the surface.

Moreover, when the lubricant starts to evaporate, it does not evaporate uniformly on the surface [9] and has faster evaporation rates in some areas. This phenomenon creates random circular zones on the lubricated surface. As a result, the proposed sensor offers a uniform sensing hotspot region to monitor the evaporation and detect the zoning effect [9].

For a better understanding of the sensor behavior, a brief circuit model is reported in Fig. 1. When the lubricant starts to evaporate, the effective permittivity in the tag resonator ambient changes. The tag is modeled with a parallel $RLC_T$, and $C_M$ is a variable capacitor to include the surface under the test, which depends on the lubricant volume on the surface. As a result, the total capacitors on the gap, $C = C_T||C_M$, will change, which creates a frequency shift in the resonance frequency $f_r$ of the tag [10]:

$$f_r = \frac{1}{\sqrt{LC}} \tag{1}$$

Since This correlation connects the lubricant evaporation process to the $f_r$ shift through the changes in $C_M$,$\Delta f_r$ is defined as the sensitivity. Assuming the lubricant evaporation in $t_1(sec)$ and $t_2(sec)$ $(t_2 > t_1)$

$$\Delta f = |f_{r2} - f_{r1}|| \approx \frac{1}{\sqrt{LC_{M2}}} - \frac{1}{\sqrt{LC_{M1}}} \tag{2}$$

where $f_{r1}$ and $C_{M1}$ are the resonance frequency and the material capacitance at $t_1$ and $f_{r2}$ and $C_{M2}$ are the resonance frequency and the material capacitance at $t_2$.

Fig. 2 presents the setup and the simulation results for $\Delta f_r$ versus $\Delta\varepsilon_r$ to demonstrate the sensitivity of the proposed design to the sample variation in two different scenarios. In scenario one, the permittivity of the LIS layer in the simulation is changed from 1.53 to 2.6 and in the second scenario, it changed from 1.97 to 2.98. In both cases, the $\Delta\ \varepsilon_r$ are the same. However, the higher initial $\varepsilon_r$ in the second scenario results in a larger smaller final $\Delta f_r$.

## III. Measurement results and analysis

Fig. 3(a) shows the fabricated sensor for evaporation monitoring; This sensor consists of a microwave reader with a ground plane and circular tag resonator. Fig. 3(b) and (c), two different lubricant-infused surfaces were tested. The first surface used a polystyrene petri dish that was first plasma treated with oxygen plasma to produce hydroxyl groups on the surface and then silanized with Trichloro (1H,1H,2H,2H-perfluorooctyl) silane (TPFS). The second surface was a dried porous bacterial nanocellulose membrane (Hydrogel) silanized with TPFS. A fluorocarbon lubricant, perfluorodecalin, was added to the two different substrates immediately before initiating measurements.

Fig. 4(a) demonstrates the measurement setup for monitoring the lubricant evaporation from the LIS. The setup includes the reader circuit and a passive sensing tag combined with the LIS. Since there is no practical approach available to measure the evaporation rate of lubricant on surfaces, proposing an inexpensive disposable sensing approach that enables monitoring evaporation in real time is the primary goal of this work. The LIS container has been selected to

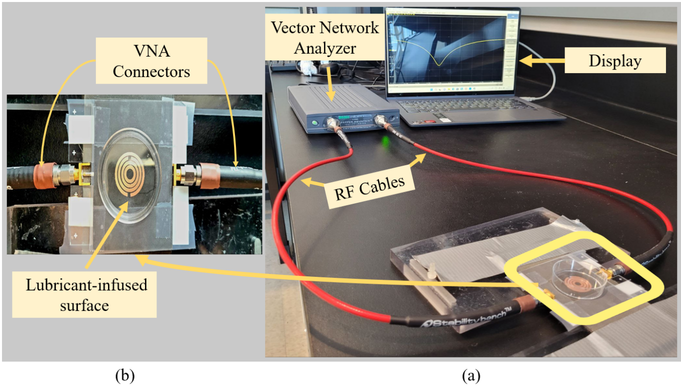


Fig. 4. Experimental setup for monitoring lubricant evaporation monitoring from LIS. The sensing platform consists of the integrated tag-LIS container, microwave reader, a Vector Network Analyzer, and a data acquisition system.

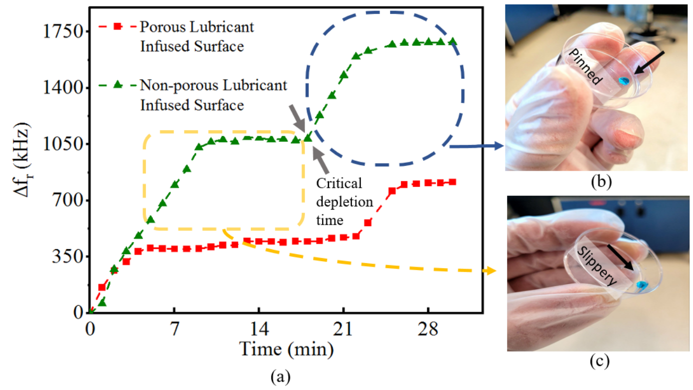


Fig. 5. Variation of $|\Delta f_r|$ over time with different phases of evaporation for porous and non-porous LIS.

cover the ring resonator tag fully. So the sample entirely overlaps with the sensing hotspot of the structure and also detects the depletion zones on the LIS in case of occurring. The M5065 Vector Network Analyzer (VNA) from Copper Mountain Technologies has been used to perform frequency measurements. LabVIEW software has been used for time-based data acquisition.

Fig. 5 displays the absolute value of resonance frequency shift during the time as a result of lubricant evaporation on both porous and non-porous samples. Due to the rapid lubricant evaporation, the frequency response is recorded every minute for 30 minutes until the lubricant was fully evaporated. After full evaporation, the frequency response shows about a 1600 kHz shift in resonance frequency for the surface without the hydrogel and about 1400 kHz frequency shift for the surface with the hydrogel. As mentioned earlier in Fig. 2, the presence of the hydrogel layer creates larger initial $\varepsilon_r$ values, resulting in a lower variation slope and more minor $\Delta f_r$ frequency shift compared to the flat non-porous petri dish samples. Since, a lower final shift is expected for hydrogel-incorporated LIS.

Different phases of evaporation are shown in Fig. 5. In the first stage, the frequency change increases very quickly as the excess lubricant on the surface evaporates. In both samples, the same volume (200 micro-liters) of lubricant was added; however, as the hydrogel is porous, more lubricant was absorbed, resulting in a lower amount of excess lubricant.

Once the lubricant layer thickness is equal to the thickness of the silane coating, the change in frequency becomes close to zero as the evaporation occurs much slower, and the lubricant becomes more stable due to van der Waals forces between the fluorine groups on TPFS and the lubricant layer. This thickness can be expressed as the critical lubricant thickness. The time to critical lubricant thickness was determined to be 10 minutes for the silanized flat petri dish and 5 minutes for the silanized hydrogel sample. A shorter time recorded for the hydrogel was due to higher lubricant absorption and less excess lubricant present on the hydrogel surface.

At this point, certain surface areas start to lose their repellency capability as the underlying substrate becomes exposed, creating a pinning point. This was verified with water droplet sliding tests. Once the lubricant is evaporated enough that the underlying solid substrate across the entire surface is exposed, the change in frequency starts to change quickly again. This can be expressed as a time to lubricant depletion, which was determined to be 17 minutes for the silanized petri dish, and 22 minutes for the silanized hydrogel. This time in both cases happens before the lubricant depletion zones occur on the exposed LIS of the tag resonator, which results in the jump in the frequency shift. This determines the critical time that the lubricant thickness is insufficient. As a result, the proposed system introduces a real-time method for lubricant effectiveness evaluation. The time to depletion was longer for the hydrogel substrate due to the porous nature giving rise to capillary forces holding the lubricant within the pores. The final plateau in the Figure represents a non-lubricated surface.

During the microwave sensing measurement, a water droplet sliding test was performed as a secondary test to verify the presence of the lubricant layer. LIS shows low water sliding angles in the presence of an intact lubricant layer. However, when the lubricant layer is depleted, the water droplets lose their mobility and pin on the surface. Therefore, the water droplet sliding is a verification that the LIS is still functioning and in a non-adhesive state (Fig. 5(b) and (c)).

## IV. Conclusion

Here, for the first time, a disposable microwave noncontact sensing platform is reported that effectively monitors the depletion of the lubricant layer over time and determines the critical lubricant thickness required for the function of a LIS. Since the evaporation of the lubricant changes the effective permittivity of the surface under the test, this variation is reflected in the recorded frequency response. The proposed design has successfully tested for monitoring evaporation in porous and non-porous LIS. It can determine the depletion trend as well as the critical depletion time, which is LIS-specific. The proposed sensor in this work is highly sensitive towards different evaporation trends that could be observed on LIS with varying lubricant retention properties and independent of surface type.

## REFERENCES


[1] M. Badv, I. H. Jaffer, J. I. Weitz, and T. F. Didar, "An omniphobic lubricant-infused coating produced by chemical vapor deposition of hydrophobic organosilanes attenuates clotting on catheter surfaces," *Scientific reports*, vol. 7, no. 1, pp. 1–10, 2017.

[2] M. Badv, F. Bayat, J. I. Weitz, and T. F. Didar, "Single and multi-functional coating strategies for enhancing the biocompatibility and tissue integration of blood-contacting medical implants," *Biomaterials*, vol. 258, p. 120291, 2020.

[3] C. Howell, T. L. Vu, C. P. Johnson, X. Hou, O. Ahanotu, J. Alvarenga, D. C. Leslie, O. Uzun, A. Waterhouse, P. Kim *et al.*, "Stability of surface-immobilized lubricant interfaces under flow," *Chemistry of Materials*, vol. 27, no. 5, pp. 1792–1800, 2015.

[4] P. Kim, M. J. Kreder, J. Alvarenga, and J. Aizenberg, "Hierarchical or not? effect of the length scale and hierarchy of the surface roughness on omniphobicity of lubricant-infused substrates," *Nano letters*, vol. 13, no. 4, pp. 1793–1799, 2013.

[5] D. C. Leslie, A. Waterhouse, J. B. Berthet, T. M. Valentin, A. L. Watters, A. Jain, P. Kim, B. D. Hatton, A. Nedder, K. Donovan *et al.*, "A bioinspired omniphobic surface coating on medical devices prevents thrombosis and biofouling," *Nature biotechnology*, vol. 32, no. 11, pp. 1134–1140, 2014.

[6] M. Shafiei, Z. Abbasi, and C. L. Ren, "Passive disposable microwave sensor for online microplastic contamination monitoring," in *2022 IEEE/MTT-S International Microwave Symposium-IMS 2022*. IEEE, 2022, pp. 263–266.

[7] Z. Abbasi, P. Shariaty, M. Nosrati, Z. Hashisho, and M. Daneshmand, "Dual-band microwave circuits for selective binary gas sensing system," *IEEE Transactions on Microwave Theory and Techniques*, vol. 67, no. 10, pp. 4206–4219, 2019.

[8] Z. Abbasi, H. Niazi, M. Abdolrazzaghi, W. Chen, and M. Daneshmand, "Monitoring ph level using high-resolution microwave sensor for mitigation of stress corrosion cracking in steel pipelines," *IEEE Sensors Journal*, vol. 20, no. 13, pp. 7033–7043, 2020.

[9] S. Peppou-Chapman and C. Neto, "Depletion of the lubricant from lubricant-infused surfaces due to an air/water interface," *Langmuir*, vol. 37, no. 10, pp. 3025–3037, 2021.

[10] H.-J. Lee, J.-H. Lee, and H.-I. Jung, "A symmetric metamaterial element-based rf biosensor for rapid and label-free detection," *Applied Physics Letters*, vol. 99, no. 16, p. 163703, 2011.